

342. Investigation of actuators with smart links

E. Kibirkštis and K. Vaitasius

Kaunas University of Technology

Studentu str. 56, LT-51424, Kaunas, Lithuania

E-mail: *edmundas.kibirkstis@ktu.lt kestutis.vaitasius@ktu.lt*

(Received 6 January 2008; accepted 17 March 2008)

Abstract. Principal schemes of actuators with smart links have been designed. Equations are presented for describing motion of a pneumatic actuator with viscous magnetorheological liquid and the vibration actuator with a smart link with shape memory. Amplitude-frequency characteristics of the vibration actuator and the pressure developed by the magnetorheological liquid vane have been determined. Application areas of the devices are proposed.

Keywords: actuator, magnetorheological fluid, shape memory, pneumatic vibroactuator

Introduction

In recent years, actuators with active links made from magnetorheological (MR) liquid or alloys with shape memory (SM) have been increasingly developed and implemented in different industries. They are used in a variety of technological equipment: suspensions of transport means [1-5], rotary mechanisms [6], vibration damping systems [7-9], various medical devices [10-12], and others [13].

Paper [1] analyzes the dynamic stability of a three-layer beam by using the incremental harmonic balance method. The impact of the static load upon the frequency of the suspension oscillations, damping factor and system stability has been determined. Paper [2] deals with the reduction of centrifugal force generated in the clutches of MR liquid actuator. The problem is solved by installing an element made from high-absorption polyurethane foam, filled with MR liquid, in the actuator construction. Paper [3] is devoted to the study of a car suspension damper and to finding an optimal solution between driver comfort and system stability. It has been determined that under harmonic excitation, the latter condition depends on the excitation frequency. A magnetic system consisting of eight independent cores has been proposed as a solution leading to optimal results in a wide range of frequencies. Methodologies for optimum design and construction of actuators with MR liquid have been presented in [4, 5]. In

paper [6] the rotary motion of a washing machine, controlled by MR clutches and breaks, is studied. Paper [7] investigates the semi-actively controlled MR liquid damper under different vibration excitation conditions. A magnetohydrostatic bearing, support and an installed damper in it with a piston made from a porous metal material are studied in [8]. Such design helps to solve the problem of MR liquid sedimentation. Paper [9] analyzes magnetic saturation of a MR liquid damper by applying finite element method. The theoretical study has been verified experimentally. Construction of a novel liquid material micro-dosing and spraying apparatus and its design optimization has been presented in the paper [10]. Paper [11] presents a knee joint training device with a MR liquid damper creating an alternating load on the joint, and discusses the results of investigation of its efficiency. An SM actuator, used as artificial muscles in a prosthesis, capable of stretching by 31,6 %, carrying a 624 g load and turning by 27 ° angle, is studied in [12]. A new area of MR liquid application has been proposed in [13]: precise polishing of glass surfaces by a polarised MR liquid jet.

The application of these actuators is predetermined by a number of their advantages: simple control, uncomplicated construction, reliability, etc. [14-19]. Paper [14] depicts the wide possibilities of applying SM alloys in smart robot systems and equipment. It has been determined that the frequency of SM actuator operation often depends on the velocity of supplying thermal power to the transducer and its removal, while this process depends on several non-

interrelated non-linear parameters. Reliability of a grip with SM alloy has been investigated in [15] and it has been found out that a wire actuator from an SM alloy can withstand over 1,175 million cycles. Paper [16] deals with a smart wire SM actuator of linear motion. The actuator operation is modeled by using the identification modeling system. The study has shown that this method can be successfully applied in modeling different SM actuators. The dependence of the behavior of the robot spring grip actuator on the cooling method, heating current and the actuator operation frequency is studied in [17]. It has been determined that the displacement amplitude increases when the heating current is increased and the frequency of the SM transformation process is reduced. Possibilities of applying SM actuators in adaptive structures, such as flexible support, etc, are studied in [18]. In [19] a hydraulic system is presented, in which four MR liquid valves without moving parts have been used. Such a solution simplifies the construction and increases its reliability. Three MR liquid models have been studied and the infinite blocking pressure model has been experimentally defined as most appropriate.

Certain characteristics of actuators with MR liquid used in microcompressors and pneumatic throttles have been studied in paper [20], while deformations of a changeable diameter throttle with SM are described in [21]. Despite the numerous studies devoted to the development and investigation of actuators mentioned above, not all their properties have been studied. The aims of the present paper are to investigate the behavior of a vibration actuator with an active SM link and to determine operating characteristics of a pneumatic actuator with MR liquid in a wide range of rotation frequencies.

Investigation of a pneumatic vibroactuator with a smart link with shape memory

The principal scheme of the actuator under study is presented in Fig. 1. The smart link with shape memory, installed in the actuator chamber, provides a possibility to enhance the functional potential of the actuator. When controlling the operation of the smart link according to a preset program, the volume of the chamber abruptly changes and so does its amplitude-frequency characteristics [22]. The ability of the smart link with shape memory to change its shape at changing temperature modes was exploited in this construction.

The deformation level and the developed strength of the smart link affect the functionality of the pneumatic transducer, therefore a model is proposed for finding these parameters. Bending $z(\xi)$ of a homogeneous bar fixed on hinges on the supports, according to Euler mathematical model, is expressed by Eq. 1:

$$z''(\xi) + FDz(\xi)\sqrt{1 - z'^2(\xi)} = 0, \tag{1}$$

where $D = \frac{1}{EI}$, E is Young's modulus, ξ is arc length,

$I = \frac{bh^3}{12}$ - inertia moment of the rectangular cross-section bar.

In our case, Young modulus is replaced by adiabatic Young's modulus [23]:

$$E_{ad} = E + E^2 \frac{T\alpha^2}{9C_p}. \tag{2}$$

The force acting upon the plate is defined by Eq. 3 [21]:

$$F = \begin{cases} SE_{ad}\alpha(T - T_0), & \text{for } T_0 \leq T < A_s, \\ S\sigma_r, & \text{for } A_s \leq T \leq A_f, \\ SE_{ad}\alpha(T - A_f), & \text{for } T > A_f, \end{cases} \tag{3}$$

where T_0 is the initial plate temperature, $S=bh$ is the area of its cross-section, and parameters A_s , A_f and σ_r are derived from mechanical stress-temperature dependence of nickel-titanium (NiTi) system alloy TN-1 [21].

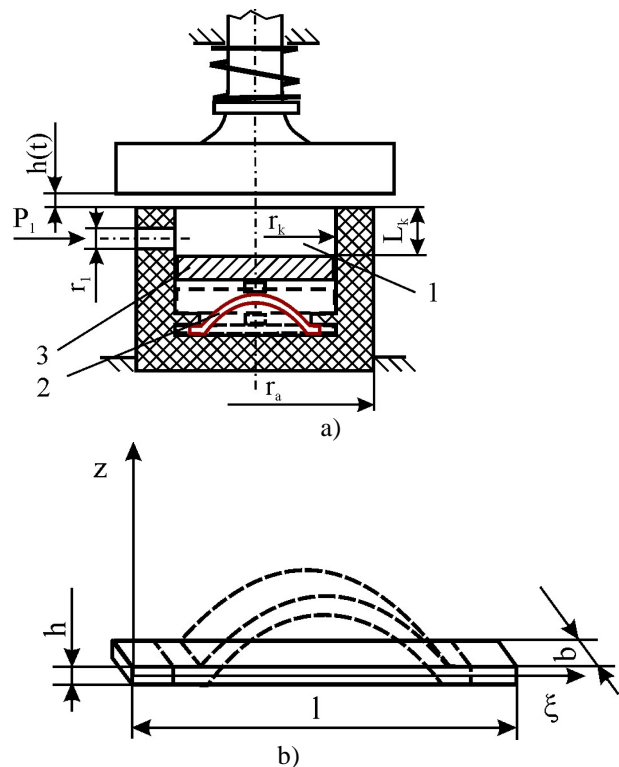


Fig. 1 Principal scheme of a pneumatic actuator with smart link with shape memory (a) and principal scheme for determination of deformation of the link (b): 1 – vibroactuator chamber, 2 – smart link with shape memory, 3 – piston, P_1 – pressure of compressed air supplied to the chamber, r_1 – radius of the air supply channel, r_k – radius of the actuator chamber, L_k – chamber height, r_a – external radius, $h(t)$ – vibration peak-to-peak swing, l , b , h – measurement of the smart link

By linearizing Eq. 1 and using Newton diagram [24], we obtain the solution which is expressed by the following formula:

$$z_k(\xi) = \frac{\sqrt{2^3} l}{k\pi} \sqrt{\frac{F - F_k}{F_k}} \sin \frac{k\pi\xi}{l} + o(\sqrt{F - F_k}), \quad (4)$$

where $F_k = \frac{k^2 \pi^2 E_{ad} I}{l^2}$, $k=1, 2, \dots$

By applying Eq. 2, Eq. 3, Eq. 5 and mechanical stress and thermal capacity dependences on temperature during direct and reverse martensitic transformations, we can calculate the critical temperatures of TN-1 alloy plate as well as the lowest possible critical strength of the plate with shape memory:

$$F_1 = \frac{\pi^2 E_{ad} I}{l^2}, \quad (6)$$

and its deformation:

$$z_1(\xi) = \frac{\sqrt{2^3} l}{\pi} \sqrt{\frac{F - F_1}{F_1}} \sin \frac{\pi\xi}{l}. \quad (7)$$

The smart link with SM installed in the chamber of the pneumatic vibrotransducer enables us to change the chamber volume suddenly thereby modifying its amplitude-frequency characteristics (see Fig. 2).

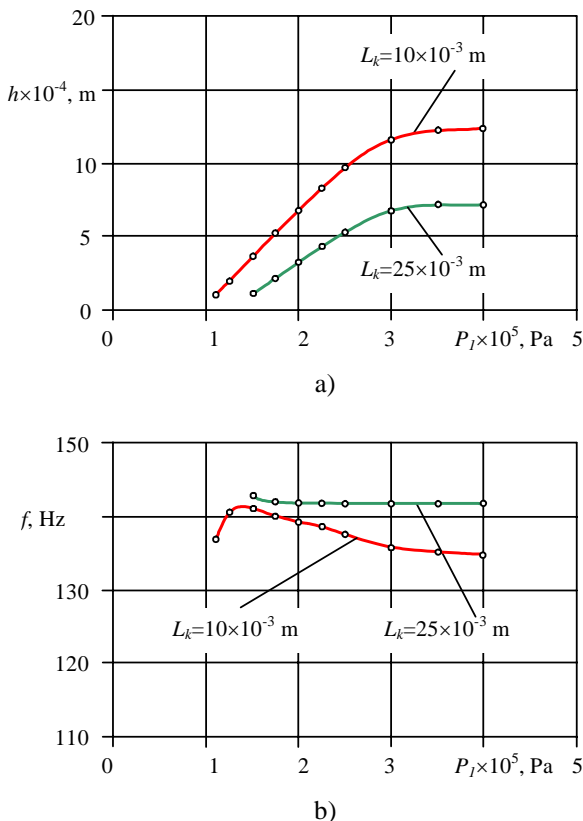


Fig. 2. Dependences of vibration peak-to-peak value (a) and frequency (b) upon the transducer chamber volume of the pneumatic vibrotransducer with a smart link with SM: $r_1=1.5 \times 10^{-3}$ m, $r_k=10 \times 10^{-3}$ m

It has been determined that when the chamber volume is larger, the vibration peak-to-peak swing is smaller, and the frequency is higher when the chamber volume is smaller (Fig. 2). In this way, the vibration zone is expanded, and in the area framed by curves 1 – 2 it is possible to abruptly change amplitude-frequency characteristics. This transducer ability to abruptly change amplitude-frequency characteristics can be employed in vibro-stands used for testing materials or devices and their vibro-treatment.

Study of pneumatic actuator with viscous magnetorheological liquid

The operation principle of the actuator drive with MR liquid under study has been presented in paper [20]. Fig. 3 illustrates a part of the general view of the drive.

In the cylindrical coordinate system, when the coordinate axis coincides with the rotor axis, the motion of viscous incompressible MR liquid vane is described by Navier-Stokes equations [25], which are expressed as follows:

$$-\frac{\partial p'}{\partial r'} + \frac{1}{Fr_m} \frac{\partial S'_m}{\partial r'} + \frac{R+r}{(R+1)^2} = 0, \quad (8)$$

$$-\frac{\partial p'}{\partial \varphi} + \frac{1}{Fr_m} \frac{\partial S'_m}{\partial \varphi} + \frac{\tau \delta (R+r')}{\rho u_0^2} = 0, \quad (9)$$

where $r' = \frac{R+r_a}{R+1}$ - is a non-dimensional relative coordinate;

$Fr_m = \frac{\rho u_0^2}{\mu_0 M_s H_*}$ - is magnetic Froude number;

$S'_m = \ln \frac{sh \xi}{\xi}$ - is a non-dimensional coordinate function of the magnetic field; ρ - is the density of the magnetic liquid, kg/m³;

$\tau = (R+r') \left[\frac{\partial^2 v}{\partial r'^2} + \frac{1}{(R+r')} \frac{\partial v}{\partial r'} - \frac{v}{(R+r')^2} \right]$;

δ - is the mean thickness of the working aperture between the rotor and the stator, m; u_0 - is the vane velocity at the stator, m/s; μ_0 - is magnetic permeability, H/m;

$M_s = \varphi_{dal} M_{so}$ - is magnetic saturation of the magnetic liquid, A/m; φ_{dal} - is the number of particles in a volume unit; M_{so} - is magnetic saturation of a particle, A/m;

$H_* = \frac{kT}{\mu_0 m}$ - is the intensity of the magnetic field, A/m; k - is Boltzmann constant; T - is temperature, K;

$m = V_{dal} M_{so}$ - is the magnetic moment of the particle; V_{dal} - is the volume of the magnetic particle, m³;

$\xi = \frac{\mu_0 m H}{kT}$ - is the argument of Langeven function; $v = u_0 v'$ - is the

azimuth component of velocity, m/s; v' - is non-dimensional velocity.

When studying the efficiency of the drive, it is important to know MR liquid pressure upon the stator surface. When $r' = 1$, the vane pressure upon the stator surface is [20]:

$$p'(1, \varphi) = p'_a + \frac{1}{Fr_m} [S'_m(1, \varphi) - S'_m(0, \varphi_a)] + \frac{1}{2} \left[1 - \left(\frac{R}{R+1} \right)^2 \right] + \frac{6(R+1)}{Re} (\varphi - \varphi_a) = \Sigma(1, \varphi) - \Sigma(0, \varphi_a) + p'_a \quad (10)$$

Performed calculations have demonstrated that the maximum pressure developed by the actuator reaches 10.8 kPa, when $n=5000$ r/min, $q=0.8$, $\delta = 2 \times 10^{-3}$.

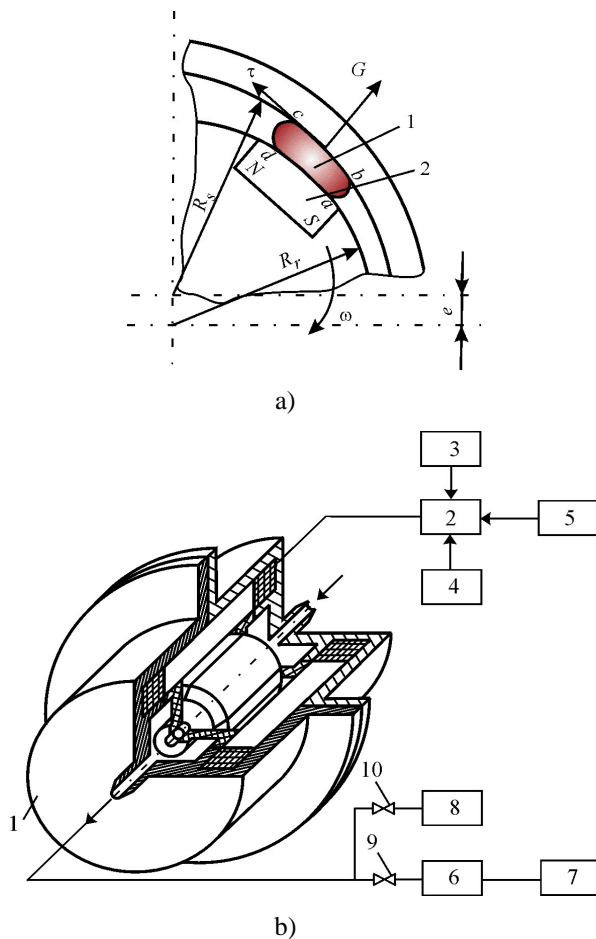


Fig. 3. Scheme of an actuator with MR liquid (a) and scheme of experimental setup for testing actuator with MR liquid (b): LV – MR liquid vane; PM – permanent magnet; a, b and c, d – free surface of MR liquid; e – eccentricity; G – centrifugal force; ω – rotor angular velocity; R_s – stator radius; R_r – rotor radius; S, N – poles of permanent magnets; τ – tangential stresses; 1 – transducer; 2 – control panel; 3, 4 – power supply; 5 – impulse generator; 6 – diaphragm; 7 – micromanometer; 8 – manometer; 9, 10 – valve

For experimental study of an actuator with MR liquid, a setup was developed (see Fig. 3, b) having the following technical parameters: the internal diameter of the stator $D_s = 18 \times 10^{-3}$ m, the external diameter of the rotor $D_r = 15 \times 10^{-3}$ m, rotor working length $L = 8 \times 10^{-3}$ m, eccentricity $e = 5 \times 10^{-5}$ m, the volume of the working chamber $V = 6 \times 10^{-7}$ m³, the number of permanent magnets is 4, the supply voltage $U = 15$ V, the supply current $I = 0.7$ A, the rotation frequency of the rotor $n = 0 \div 5000$ r/min, $M_s = 51.7$ kA/m, $\rho = 1585$ kg/m³, the diameter of magnetic particles $R_{dal} = 9.01 \times 10^{-9}$ m.

The experimental set-up was also used for determination of the values of the pressure and efficiency generated by the transducer. When the transducer rotor with the magnetic liquid vanes is rotating, the pressure difference developed in diaphragm 6 (see Fig. 3, b) is registered by micromanometer. According to the manometer readings, the pressure and the efficiency developed by the transducer are calculated. The developed pressure difference in the system is determined by the the following expression [25]:

$$\Delta p = l_{mat} K_p g \quad (11)$$

where l_{mat} is the height of the liquid rise in the micromanometer; K_p - is the coefficient evaluating the declination angle of the manometer tube; g - free fall acceleration.

The efficiency of the transducer is determined by the formula:

$$Q = \frac{\alpha \varepsilon \pi d_0^2}{4 \sqrt{2 \Delta p / \rho_o}}, [m^3 / s]$$

where α - is the coefficient depending on the diameter of the diaphragm and the parameters of the measured medium; ε is correction coefficient; d_0 is the diameter of the diaphragm inlet channel; ρ_o is the gas (air) density.

The dependence of the pressure generated by the transducer on the MR liquid vane filling coefficient while changing the rotation frequency is given in Fig. 4, a. Presented curves indicate that the value of the pressure generated by the actuator directly depends on the MR liquid vane filling coefficient and the rotation frequency. The highest pressure value is obtained when MR liquid filling coefficient is close to 0.9. The generated pressure increases with increasing rotation frequency (up to 13.7 kPa, when $n=4615$ r/min).

Fig. 4, b illustrates the dependence of the transducer efficiency upon MR liquid vane filling coefficient, while changing the rotation frequency of the rotor.

Research results indicate that the transducer capacity also depends on the rotation frequency of the rotor and MR liquid vane filling coefficient. However, only at low

rotation frequencies of the rotor (up to 2000 r/min), the capacity rises gradually with changing MR liquid vane filling coefficient. The maximum achieved value of the efficiency is $0.37 \times 10^{-6} \text{ m}^3/\text{s}$.

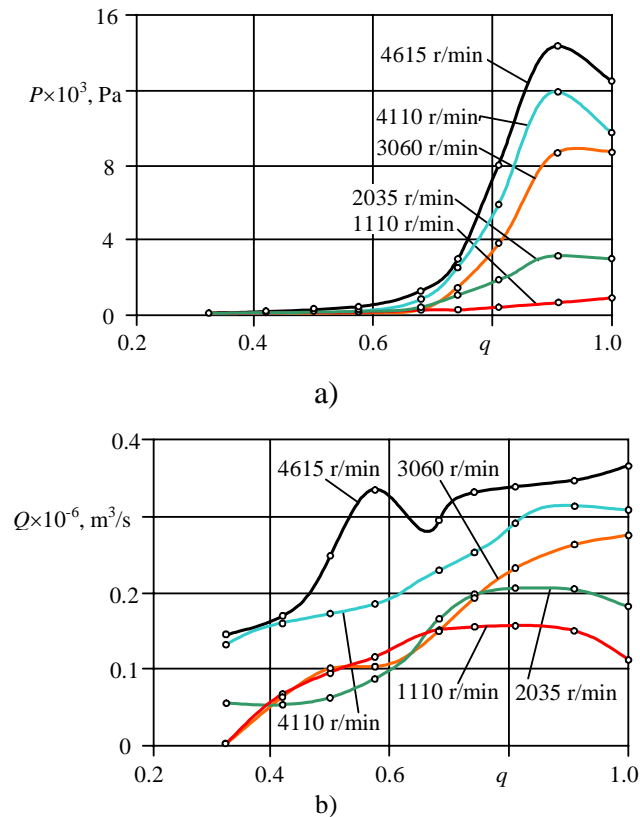


Fig. 4. Dependence of pressure p (a) and efficiency Q (b) generated by the transducer upon the MR liquid vane filling coefficient q while changing the rotor rotation frequency n

Conclusions

The investigation of the transducer with SM has led to the conclusion that:

1. Formulas have been presented which enable us to determine the deformation of the smart link with SM (plate) and the critical strength during the martensitic transformations in the link.

2. Introduction of a smart link with SM in the vibrotransducer expands its application area since it enables abrupt modification of the amplitude-frequency characteristics of the actuator.

The performed study of the actuator with MR liquid leads to the following conclusions:

1. The value of the pressure generated by the transducer actuator depends directly on MR liquid vane filling coefficient and rotation frequency. The highest pressure value is obtained when MR liquid filling coefficient is close to 0.9. The pressure rises with increase in rotation frequency (up to 13.7 kPa, when $n=4615$ r/min).

2. The efficiency developed by the transducer also depends on the rotation frequency of the rotor and on MR

liquid vane filling coefficient. The maximum obtained efficiency value is $0.37 \times 10^{-6} \text{ m}^3/\text{s}$.

3. At low MR liquid vane filling coefficient q values – up to 0.67 – unstable operating zones of the transducer caused by hermetic flaws of the system have been observed.

4. Findings of the performed theoretical and experimental study are sufficiently adequate. Obtained pressure values do not exceed 15%.

References

1. **Yeh Z.F., Shih Y.S.** Dynamic characteristics and dynamic instability of magnetorheological material-based adaptive beams // *Journal of Composite Materials*, 2006, Vol. 40, No. 15, p. 1333-1359.
2. **Neelakantan V.A., Washington G.N.** Modeling and reduction of centrifuging in magnetorheological (MR) transmission clutches for automotive applications // *Journal of Intelligent Material Systems and Structures* 2005, Vol. 16, No. 9, p. 703-711.
3. **Sassi S., Cherif K., Mezghami L., Thomas M., Kotrane A.** An innovative magnetorheological damper for automotive suspension: from design to experimental characterization // *Smart Materials & Structures* 2005, Vol.14, No. 4, p. 811-822.
4. **Carlson J.D.** MR fluids and devices in the real world // *International Journal of Modern Physics B*, 2005, Vol. 19, Iss. 7/9, p. 1463-1470.
5. **Tian L., Wang Y.** Study on power transmission technology based-on MRF // *International Journal of Modern Physics B*, 2005, Vol. 19, Iss. 7/9, p. 1563-1569.
6. **Choi S.B., Lee Y.** Rotational motion control of a washing machine using electrorheological clutches and brakes // *Proceedings of the Institution of Mechanical Engineers, Part C: Journal of Mechanical Engineering Science*, 2005, Vol. 219, No. 7, p. 627-637.
7. **Dominguez A., Sedaghati R., Stiharu I.** A new dynamic hysteresis model for magnetorheological dampers // *Smart Materials & Structures*, 2006, Vol. 15, No. 5, p. 1179-1189.
8. **Guldbake J.M., Hesselbach J.** Development of bearings and a damper based on magnetically controllable fluids // *Journal of Physics: Condensed Matter*, 2006, Vol. 18, No. 38, p. S2959-S2972.
9. **Zhang H.H., Liao C.R., Chen V.M., Huang S.L.** A magnetic design method of MR fluid dampers and FEM analysis on magnetic saturation // *Journal of Intelligent Material Systems and Structures*, 2006, Vol. 17, No 8-9, p. 813-818.
10. **Palevicius A., Ragulskis K., Bubulis A., Ostasevicius V., Ragulskis M.** Development and operational optimization of micro spray system // *Smart Structures and Materials 2004: Smart Structures and Integrated Systems* 5390: p. 429-438.
11. **Dong S.F., Lu K.Q., Sun J.Q., Rudolph K.** Rehabilitation device with variable resistance and intelligent control // *Medical Engineering & Physics* 2005, Vol. 27, Iss. 3, p. 249-255.
12. **Price A., Edgerton A., Cocaud C., Naguib H., Jnifene A.** A study on the thermomechanical properties of shape memory alloys-based actuators used in artificial muscles // *Journal of Intelligent Material Systems and Structures*, 2007, Vol. 18, No. 1, p. 11-18.

13. **Tricard M., Kordonski W.L., Shorey A.B.** Magnetorheological jet finishing of conformal, freeform and steep concave optics // *Cirp Annals: Manufacturing Technology*, 2006, Vol. 55, No. 1, p. 309-312.
14. **Sreekumar M., Nagarajan T., Singaperumal M., M. Zoppi, R. Molfino.** Critical review of current trends in shape memory alloy actuators for intelligent robots // *Industrial Robot: An International Journal*, 2007, Vol. 34, No. 4, p. 285-294.
15. **Zhong Z.W., Chan S.Y.** Investigation of a gripping device actuated by SMA wire // *Sensors and Actuators A: Physical*, 2007, Vol. 136, Iss. 1, p. 335-340.
16. **Khidir E.A., Mohamed N.A., Nor M.J.M., Mustafa M.M.** A new concept of a linear smart actuator // *Sensors and Actuators A: Physical* 2007, Vol. 135, Iss. 1, p. 244-249.
17. **Yan S.Z., Liu X.J., Xu F., Wang J.H.** A gripper actuated by a pair of differential SMA springs // *Journal of Intelligent Material Systems and Structures*, 2007, Vol. 18, No. 5, p. 459-466.
18. **Da Silva E.P.** Beam shape feedback control by means of a shape memory actuator // *Materials & Design*, 2007, Vol. 28, Iss. 5, p. 1592-1596
19. **Yoo J.H., Wereley N.M.** Performance of a magnetorheological hydraulic power actuation system // *Journal of Intelligent Material Systems and Structures*, 2004, Vol. 15, No. 11, p. 847-858.
20. **Bansevičius R., Kibirkštis E., Vaitasius K. and Kabelkaitė A.** Magnetorheological Liquid Actuators // 9th International Conference on New Actuators 2004, p. 613 – 616.
21. **Kibirkštis E., Liaudinskas R., Stupelis L.** Theoretical Studies of Adaptive Transducers with Specific Properties. Application to Shape Memory Material // *Materials science*, 1999, No. 1(8), p. 23-26.
22. **Bansevičius R.P., Kibirkštis E., Vaitasius K.** Study of Pneumatic Vibrotransducers. *Mechanics*, 2003, No. 3(41), p. 40-47.
23. **Landau L.D., Lifshits E.M.** *Theory of Elasticity*. Moscow, Nauka, 1965. (in Russian).
24. **Vainberg M.M., Trenogin V.A.** *Theory of Branching of nonlinear equations*. Moscow, Nauka, 1969. (in Russian).
25. **Encyclopedia of fluid mechanics.** Flow phenomena and measurement. Vol. 1. Gulf Publishing Company, 1986, p. 277-281.